Journal of Southeast University (English Edition) Vol. 28, No. 4, pp. 445 - 450 Dec. 2012 ISSN 1003—7985

Image edge detection based on nonsubsampled contourlet transform and mathematical morphology

He Kunxian[1] Wang Qing[1] Xiao Yanchang[1] Wang Xiaobing[2]

([1] School of Instrument Science and Engineering, Southeast University, Nanjing 210096, China)
([2] Firing Office, Nanjing Artillery Academy, Nanjing 211132, China)

Abstract: A novel algorithm for image edge detection is presented. This algorithm combines the nonsubsampled contourlet transform and the mathematical morphology. First, the source image is decomposed by the nonsubsampled contourlet transform into multi-scale and multi-directional sub-bands. Then the edges in the high-frequency and low-frequency sub-bands are respectively extracted by the dual-threshold modulus maxima method and the mathematical morphology operator. Finally, the edges from the high-frequency and low-frequency sub-bands are integrated to the edges of the source image, which are refined, and isolated points are excluded to achieve the edges of the source image. The simulation results show that the proposed algorithm can effectively suppress noise, eliminate pseudo-edges and overcome the adverse effects caused by uneven illumination to a certain extent. Compared with the traditional methods such as LoG, Sobel, and Canny operators and the modulus maxima algorithm, the proposed method can maintain sufficient positioning accuracy and edge details, and it can also make an improvement in the completeness, smoothness and clearness of the outline.

Key words: image edge detection; nonsubsampled contourlet transform (NSCT); modulus maxima; dual-threshold; mathematical morphology; structural elements

doi: 10.3969/j. issn. 1003 - 7985. 2012. 04. 013

Image edge detection is one of the most important steps in image processing, analysis and pattern recognition systems. Its importance arises from the fact that the edges often provide an indication of the physical extent of an object within an image. The sufficient information of a characteristic feature is provided by the detection of edges because the size of the image data is reduced to a size that is more suitable for image analysis. The performance of the later stages to identify objects depends on the success of the edge characterization step. In general, the following goals must be considered during the process of detecting edges: An edge should not be missed or non-edge should not be marked as an edge, and the edge should be located at correct position.

Early image edge detection methods employed local operators to approximately compute the first derivative of the gray-level gradient of an image in the spatial domain. The locations of the local maxima of the first derivative are considered to be edge points. Classical image edge detection operators are examples of the gradient-based image edge detector, such as the LOG operator, the Sobel operator, the Canny operator, etc. Since they are very sensitive to noise, classical image edge detection operators are not practical in real image processing. Recently, there have been many previous works on detecting the edges of the image which is corrupted by noise by using different methods, such as the wavelet transform method[1-2], the mathematical morphological method[3-5], and the modulus maximum method [6], etc.

The contourlet transform (CT) was developed as a true two-dimensional representation for images that can efficiently capture the intrinsic geometrical structure of pictorial information[7]. Because of the employment of the directional filter banks (DFB), the CT can provide a much more detailed representation of natural images with abundant textural information than wavelets. However, shift-variance is an important weakness of CT. So, the NSCT is developed and some applications are studied [8-9].

If improper fixed thresholds were selected, pseudo-edges were detected in the traditional NSCT. The dual-threshold method was employed to avoid this question and it was proved to be effective [10]. There is much edge information in the low-frequency sub-band, which can be detected by a mathematical morphology operator.

This article describes the theory of nonsubsampled contourlet transform and mathematical morphology, and their applications in image edge detection. Then, a new edge detection algorithm is produced by the fusion of the two methods. Finally, MATLAB simulations are carried out to verify the theoretical analysis and the correctness of the new algorithm.

Received 2012-04-19.

Biographies: He Kunxian (1979—), male, graduate; Wang Qing (corresponding author), male, doctor, professor, 3398a@263. net.

Foundation items: The National Key Technologies R&D Program during the 12th Five-Year Period of China (No. 2012BAJ23B02), Science and Technology Support Program of Jiangsu Province (No. BE2010606).

Citation: He Kunxian, Wang Qing, Xiao Yanchang, et al. Image edge detection based on nonsubsampled contourlet transform and mathematical morphology[J]. Journal of Southeast University (English Edition), 2012, 28(4): 445 - 450. [doi: 10.3969/j. issn. 1003 - 7985. 2012. 04. 013]

1 Nonsubsampled Contourlet Transform

NSCT is a flexible multi-scale, multi-directional, and shift-invariant image decomposition method. An original image can be decomposed into a low-frequency sub-band and high-frequency sub-bands with this method. The high-frequency sub-band is decomposed into some directional sub-bands. Repeating the above operation for the low-frequency sub-band, multi-scale and multi-directional image decompositions can be achieved.

Fig. 1 (a) displays an overview of the proposed NSCT. The structure consists of a bank of filters that splits the two-dimensional frequency plane in the sub-bands illustrated in Fig. 1 (b). The proposed transform can thus be divided into two shift-invariant parts: 1) a nonsubsampled pyramid (NSP) structure that ensures the multi-scale property and 2) a nonsubsampled DFB (NSDFB) structure that gives directionality.

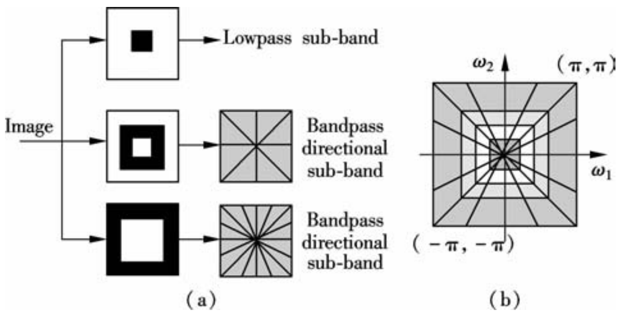

Fig. 1 Nonsubsampled contourlet transform. (a) NSFB structure that implements the NSCT; (b) Idealized frequency partitioning obtained by the proposed structure

1.1 Nonsubsampled pyramid (NSP)

The multi-scale property of the NSCT is obtained from a shift-invariant filtering structure that achieves a sub-band decomposition similar to that of the Laplacian pyramid. This is achieved by using two-channel nonsubsampled 2-D filter banks. Fig. 2 illustrates the proposed nonsubsampled pyramid (NSP) decomposition with three stages.

To meet the perfect reconstruction, the NSP provided by the filters needs to satisfy the Bezout identity:

$$H_0(z)G_0(z)+H_1(z)G_1(z)=1$$

where $H_0(z)$ is a low-pass decomposition filter; $H_1(z)$ is a high-pass decomposition filter; $G_0(z)$ is a low-pass reconstruction filter; $G_1(z)$ is a high-pass reconstruction filter.

At the core of the proposed NSCT structure is the 2-D two-channel NSFB. As shown in Fig. 3, the pyramid NSFB is needed to construct the NSCT. Through this set of filters, the image is divided into a low-frequency sub-band and high-frequency sub-bands. The multi-scale image can be achieved by iterating the filtered low-frequency sub-band.

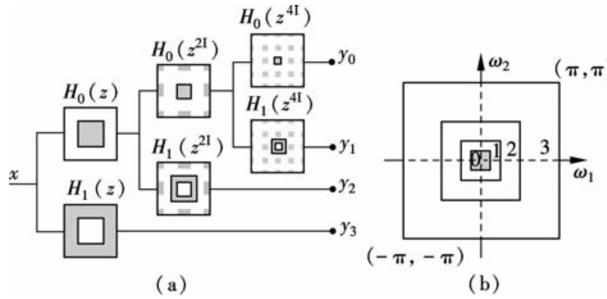

Fig. 2 2-D multi-resolution expansion. (a) Three-stage pyramid decomposition; (b) Sub-bands on the 2-D frequency plane

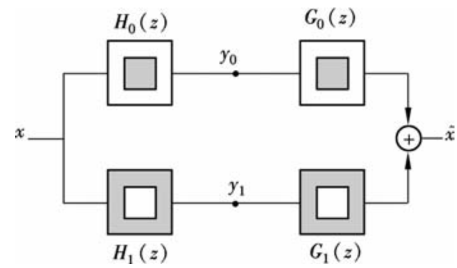

Fig. 3 Pyramid NSFB

1.2 Nonsubsampled directional filter bank (NSDFB)

A shift-invariant directional expansion is obtained by a NSDFB. The NSDFB is constructed by eliminating the down-samplers and up-samplers in the DFB. This is done by switching off the down-samplers/up-samplers in each two-channel filter bank in the DFB tree structure and up-sampling the filters accordingly. Fig. 4 illustrates a four-channel decomposition.

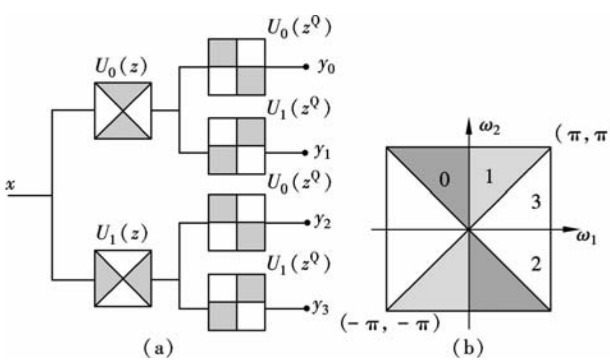

Fig. 4 Four-channel nonsubsampled directional filter bank constructed with two-channel fan filter banks. (a) Filtering structure; (b) Corresponding frequency decomposition

2 Detecting Edges in High-Frequency Sub-Bands

2.1 Modulus maxima algorithm

The modulus maxima algorithm is used to process the high-frequency sub-bands[5]. Fig. 5 illustrates eight directions in the sub-band decomposed by the NSDFB, and eight directions are equivalent to the gradient direction of the $\arg C_{j,k}^{(l)}$ directional edge at each point $C_{j,k}^{(l)}(n)$ of the sub-band. The local maxima value can be determined by comparing the modulus values of two adjacent elements in the corresponding equivalent gradient direction $\arg(\mathrm{grad}\,C_{j,k}^{(l)})$ of mod $[C_{j,k}^{(l)}(n)]$ and $\arg C_{j,k}^{(l)}(n)$ as follows:

$$\mathrm{mod}[C_{j,k}^{(l)}(n_1, n_2)] = \begin{cases} 0 & \mathrm{mod}[C_{j,k}^{(l)}(n_1, n_2)] < \\ & \quad \mathrm{mod}[C_{j,k}^{(l)}(n_1 - r_1(n_1), n_2 - r_1(n_2))] \\ 0 & \mathrm{mod}[C_{j,k}^{(l)}(n_1, n_2)] < \\ & \quad \mathrm{mod}[C_{j,k}^{(l)}(n_1 - r_2(n_1), n_2 - r_2(n_2))] \\ \mathrm{mod}[C_{j,k}^{(l)}(n_1, n_2)] & \text{others} \end{cases} \tag{2}$$

where $r(n_1)$ and $r(n_2)$ represent, respectively, the horizontal and vertical coordinates offset obtained by comparing $C_{j,k}^{(l)}(n)$ with n in the direction of $\arg(\mathrm{grad}C_{j,k}^{(l)})$.

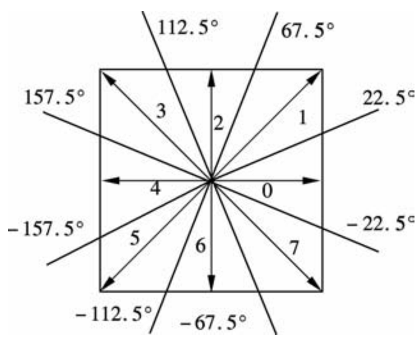

Fig. 5 Equivalent gradient directions in directional sub-band

2.2 Detecting high-frequency edge with dual-threshold method

According to Ref. [6], high-frequency sub-bands are processed by thresholds τ_1 and τ_2 ($\tau_2 = \alpha\tau_1$; α is the scale factor; τ_1 is the low threshold and τ_2 is the high threshold.), respectively, and corresponding edge matrices $\boldsymbol{T}_1$ and $\boldsymbol{T}_2$ are achieved.

The specific steps are as follows:

1) When scanning in the matrix $\boldsymbol{T}_2$, if a non-zero pixel P is encountered, the contour is tracked from the starting point P to the end point Q of the contour.

2) When scanning in the eight neighborhoods of the reference point Q in the matrix $\boldsymbol{T}_1$, if a non-zero pixel R is encountered, R is included to $\boldsymbol{T}_2$ as an edge point of the contour in the matrix $\boldsymbol{T}_1$. Return to step 1 from the point R until this scanning cannot be continued in $\boldsymbol{T}_1$ and $\boldsymbol{T}_2$.

3) The contour is marked to be accessed after the contour that contains the point P is linked in the two matrices, turn back to step 1 to find the next contour. The operation from step 1 to step 3 is repeated until a new contour cannot be found. When an isolated non-zero point in the search process is encountered, it is set to zero.

3 Detecting Edges in Low-Frequency Sub-Band

The mathematical morphology is composed by a series of morphological algebraic arithmetic operators. The basic morphological operations, namely, erosion, dilation, opening, and closing etc. are used for detecting, modifying, and manipulating the features presented in the image based on their shapes. The shapes and the sizes of the structural elements (SE) play crucial roles in such a type of processing and are, therefore, chosen according to the needs and purposes of the associated application.

Next, some basic mathematical morphology operators of gray-scale images are introduced.

In the two-dimensional Euclidean space Z^2, let $F(x, y)$ denote a gray-scale two-dimensional image, and B denote SE. The dilation of a gray-scale image $F(x, y)$ by a gray-scale SE $B(s, t)$ is denoted as

$$(F \oplus B)(x, y) = \max\{F(x - s, y - t) + B(s, t)\} \tag{3}$$

The erosion of a gray-scale image $F(x, y)$ by a gray-scale SE $B(s, t)$ is denoted as

$$(F \Theta B)(x, y) = \min\{F(x + s, y + t) + B(s, t)\} \tag{4}$$

The opening and closing of a gray-scale image $F(x, y)$ by gray-scale SE $B(s, t)$ are denoted, respectively, as

$$F \circ B = (F \Theta B) \oplus B \tag{5}$$

$$F \cdot B = (F \oplus B) \Theta B \tag{6}$$

The edge of image $F(x, y)$, $E_d(F)$, is defined as the difference set of the dilation domain of $F(x, y)$ and the domain of $F(x, y)$. This is also known as the dilation residue edge detector:

$$E_{\mathrm{d}}(F) = (F \oplus B) - F \tag{7}$$

Accordingly, the edge of image $F(x, y)$, which is denoted by $E_{\mathrm{e}}(F)$, can also be defined as the difference set of the domain of $F(x, y)$ and the erosion domain of $F(x, y)$. This is also known as the erosion residue edge detector:

$$E_{\mathrm{e}}(F) = F - (F \Theta B) \tag{8}$$

The dilation and erosion are often used to compute the morphological gradient $E(F)$ of image $F(x, y)$, which is expressed as

$$E(F) = (F \oplus B) - (F \Theta B) \tag{9}$$

The morphological gradient highlights a sharp gray-level transition in the input image, and therefore, it is often used as an edge detector.

In this paper, several kinds of SEs are chosen, and the direction angles of all the line SEs are 0°, 45°, 90°, 135° in the 5 × 5 square window. And other SEs are shown as follows:

$$\begin{bmatrix} 0 & 1 \\ 1 & 1 \end{bmatrix} \quad \begin{bmatrix} 1 & 0 \\ 1 & 1 \end{bmatrix} \quad \begin{bmatrix} 1 & 1 \\ 0 & 1 \end{bmatrix} \quad \begin{bmatrix} 1 & 1 \\ 1 & 0 \end{bmatrix}$$

$$\begin{bmatrix} 0 & 1 & 0 \\ 1 & 1 & 1 \\ 0 & 1 & 0 \end{bmatrix} \quad \begin{bmatrix} 1 & 0 & 0 & 1 \\ 0 & 1 & 1 & 0 \\ 0 & 1 & 1 & 0 \\ 1 & 0 & 0 & 1 \end{bmatrix}$$

where "1" denotes the components of SE.

4 The Algorithm and Implementation Steps

The specific algorithm is described as follows:

1) The image is decomposed into two parts of the low-frequency and high-frequency images using the NSCT.

2) The high-frequency edges of the image are detected by the modulus maxima algorithm. First, the low-frequency coefficients are set to zero, and $C_{j,k}^{(l)}$ remain unchanged. And then the modulus maxima algorithm is used to detect the edges of the high-frequency sub-bands in each scale, and the dual-threshold method compensates for the link to obtain the edge matrix. Finally, the high-frequency edge of the image is achieved by the inverse NSCT.

3) The low-frequency edges of the image are detected by the mathematical morphology. A mathematical morphology operator is used to detect the edges of the low-frequency sub-band, and then the low-frequency edge of the image is achieved.

4) The high-frequency and low-frequency edge images are fused and refined. The effective edge image can be received by adding high-frequency to low-frequency due to the shift-invariance of the NSCT. Finally, the image is refined into a single pixel edge image and isolated points are excluded.

5 Experimental Results and Analysis

In the experiment, the source images (aerial and Barbara) are decomposed with three stages by dmaxflat NSDFB and 9-7 NSP of the proposed algorithm with Matlab 2007b in this paper, and then eight directions are decomposed in each high-frequency sub-band. For the aerial image, the low-threshold is set to 20 in the dual-threshold method, and then the high-frequency is 1.8 times the low-threshold.

Fig. 6 illustrates six images. Fig. 6(a) is the original aerial image. Figs. 6(b) to (d) are the edge images detected by the LoG operator, the Sobel operator, and the Canny operator, respectively. Fig. 6(e) is the edge image detected by the method proposed in Ref. [10], and Fig. 6(f) is the edge image detected by the method proposed in this paper. Tab. 1 shows the experimental results of the aerial image.

Fig. 7 illustrates six images. Fig. 7(a) is the original Barbara image. Figs. 7(b) to (d) are the edge images detected by the LoG operator, the Sobel operator, and the Canny operator, respectively. Fig. 7(e) is the edge image detected by the method proposed in Ref. [10], and Fig. 7(f) is the edge image detected by the method proposed in this paper. Tab. 2 shows the experimental results of the Barbara image.

The simulation results (see Fig. 6(f) and Fig. 7(f)) show that the proposed algorithm can detect the accurate positioning details of the edges, clear texture, complete and coherent outlines and overcome the adverse effects caused by uneven illumination to a certain extent. Better visual effects can be achieved.

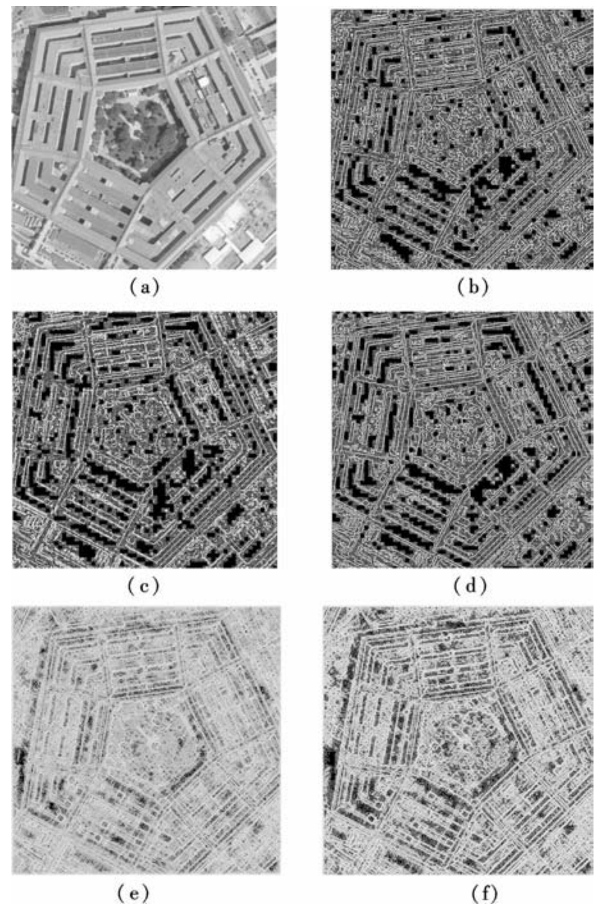

Fig. 6 Edge detection results of aerial image. (a) Origin; (b) LoG operator; (c) Sobel operator; (d) Canny operator; (e) Ref. [10]; (f) This paper

Tab. 1 Experimental results of aerial image

Index	LoG operator	Sobel operator	Canny operator	Ref. [10]	This paper
Number	31 983	32 122	35 370	42 468	79 895
Continuity	General	Poor	Better	Good	Better
Accuracy	General	Good	General	Better	Better
Smoothness	Poor	Good	Good	Good	Better
Time/s	0.61	0.32	1.25	547	560

From the results of several algorithms in the aerial image, the LoG operator can detect lots of edge points, but there are many false edges and noise points (see Fig. 6(b)); at the same time, it is almost the worst one of several algorithms from the visual effects. The edges detected by the Sobel operator are smooth and their positioning is accurate, but there is some loss in the details and some fracture in the outlines. The Canny operator can obtain good detection results in the outline, but many details cannot be detected. The algorithm proposed in Ref. [10] can detect the accurate details of the edge, complete and coherent outlines. The algorithm proposed in this paper can effectively suppress noise, eliminate pseudo-edges, and detect clear, complete and coherent outlines.

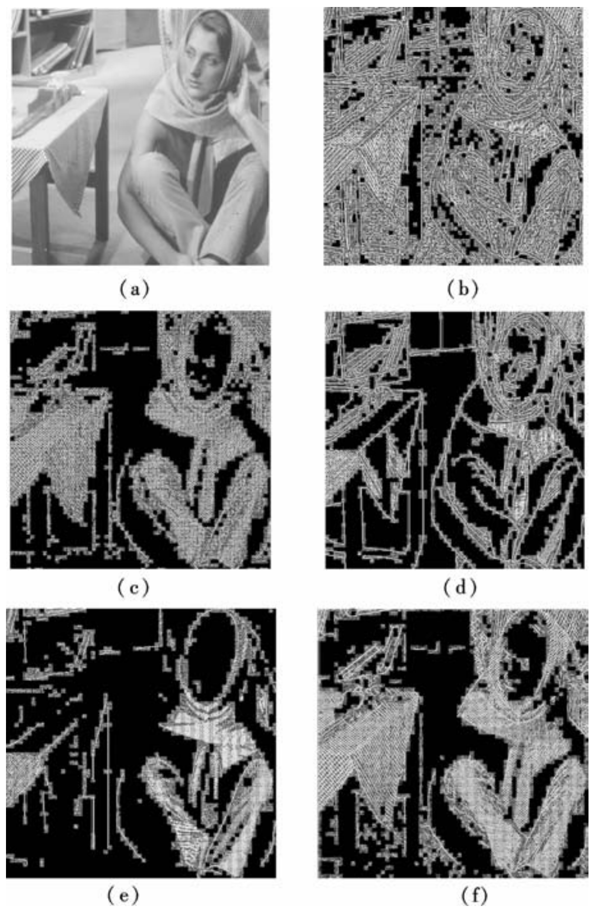

Fig. 7 Edge detection results of Barbara image. (a) Origin; (b) LoG operator; (c) Sobel operator; (d) Canny operator; (e) Ref. [10]; (f) This paper

Tab. 2 Experimental results of Barbara image

Index	LoG operator	Sobel operator	Canny operator	Ref. [10]	This paper
Number	35 214	14 869	19 760	24 695	39 778
Continuity	Poor	General	Better	Good	Good
Accuracy	General	Good	General	Better	Better
Smoothness	Poor	Good	Better	Good	Good
Time/s	0. 51	0. 30	1. 10	491	525

The robustness of the new algorithm is verified by the simulation results in the Barbara image. Furthermore, the new algorithm can efficiently detect more details in the area of uneven illumination, and work better for the image with regular structures.

6 Conclusion

The novel algorithm proposed in this paper combines the NSCT and mathematical morphology. The NSCT can effectively express the image with multi-scale and multi-directional decomposition and translation invariance. The mathematical morphology can extract abundant structural information of the image content. The new fused method not only achieves accurate positioning, but also suppresses noise, eliminates pseudo-edges and overcomes the adverse effects caused by uneven illumination to a certain extent. Furthermore, this method makes preparation for succeeding image processing.

References

[1] Mallat S, Zhong Sifen. Characterization of signals from multiscale edges[J]. *IEEE Transactions on Pattern Analysis and Machine Intelligence,* 1992, **14**(7): 710 – 732.

[2] Tao Hongjiu, Liu Jian, Tian Jinwen. Remote sense image edge detection based on wavelet transform and mathematical morphology [J]. *Infrared and Laser Engineering,* 2002, **31**(2): 154 – 157. (in Chinese)

[3] Haralick R M, Sternberg S R, Zhuang Xinhua. Image analysis using mathematical morphology[J]. *IEEE Transactions on Pattern Analysis and Machine Intelligence,* 1987, **9**(4): 532 – 550.

[4] Zhao Yuqian, Gui Weihua, Chen Zhencheng. Edge detection based on multi-structure elements morphology [C]//*Proceedings of the 6th World Congress on Intelligent Control and Automation.* Dalian, China, 2006: 9795 – 9798.

[5] Huang Hailong, Wang Hong, Guo Fan, et al. A multi-shape and multi-scale edge detection algorithm based on mathematical morphology [J]. *Journal of Northeastern University: Natural Science*, 2010, **31**(10): 1483 – 1486. (in Chinese)

[6] Zhang Y T, Yin Z K, Wang J Y. A new image edge detection scheme [J]. *Journal of Electronics & Information Technology,* 2008, **30**(6): 1295 – 1299. (in Chinese)

[7] Do M N, Vetterli M. The contourlet transform: an efficient directional multiresolution image representation[J]. *IEEE Transactions on Image Processing,* 2005, **14**(12): 2091 – 2106.

[8] Da Cunha A L, Zhou Jianping, Do M N. Nonsubsampled contourlet transform: filter design and applications in denoising[C]//*Proc of the IEEE International Conference on Image Processing.* Genova, Italy, 2005: 1749 – 1752.

[9] Da Cunha A L, Zhou Jianping, Do M N. The nonsubsampled contourlet transform: theory, design, and application [J]. *IEEE Transactions on Image Processing,* 2006, **15**(10): 3089 – 3101.

[10] Xiao Yihan, Xi Zhihong, Hai Tao, et al. Image edge detection based on nonsubsampled contourlet transform [J]. *Systems Engineering and Electronics,* 2011, **33**(7): 1668 – 1672. (in Chinese)

基于非下采样轮廓波变换与数学形态学方法的图像边缘检测

何坤贤[1]　王　庆[1]　肖彦昌[1]　王晓兵[2]

([1]东南大学仪器科学与工程学院，南京 210096)
([2]南京炮兵学院射击教研室，南京 211132)

摘要:提出了一种新的图像边缘检测算法,该算法融合了非下采样轮廓波变换与数学形态学方法来实现图像的边缘检测.首先,源图像被非下采样轮廓波变换分解成多尺度、多方向子带;然后,分别采用双阈值模极大值算法和数学形态学方法提取高频与低频子带的边缘信息;最后,综合高频、低频子带边缘信息,得到源图像全部的边缘信息,并进行细化,剔除孤立点,获得源图像的边缘.仿真实验结果表明:新算法能够有效抑制噪声,去除伪边缘,一定程度上克服了光照不均引起的不良影响;与传统经典算法 LoG,Sobel 和 Canny 及模极大值方法相比,该算法能保持足够的定位精度和边缘细节,且边缘轮廓的完整性、光滑度、清晰度等得到明显提升.

关键词:图像边缘检测;非下采样轮廓波变换;模极大值;双阈值;数学形态学;结构元素

中图分类号:TP391.41